Face-dependent Hamaker constants and surface melting or nonmelting of noncubic crystals

Andrea Dal Corso
International School for Advanced Studies (SISSA-ISAS), Via Beirut 2/4, I-34014 Trieste, Italy

Erio Tosatti
International School for Advanced Studies (SISSA-ISAS), Via Beirut 2/4, I-34014 Trieste, Italy
and International Center for Theoretical Physics (ICTP), P.O. Box 596, I-34014 Trieste, Italy
(Received 4 November 1992)

Surface melting is strongly influenced by long-range dispersion forces which crucially control the thickness l of the liquid layer that forms at the crystal surface, through a free-energy term of asymptotic form $V(l)=H/l^2$. In isotropic crystals, the face-independent Hamaker constant H is usually calculated by a well-known formula by Lifshitz *et al.* that relates dispersion forces to the optical conductivity of the solid and the liquid. In this paper we generalize this result to anisotropic crystals specializing in uniaxial crystal surfaces normal or parallel to the optical c axis, and to surfaces of orthorhombic biaxial crystals normal to one principal axis. The main result is that the Hamaker constant becomes face dependent, and may, in principle, even change sign from one face to another. Using experimental data for frequency-dependent dielectric constants we have calculated Hamaker constants of the main faces for some low-melting-point anisotropic metals, namely, α-Ga, β-Sn, and Cd. It is found that H is negative and large for all faces of α-Ga, implying surface nonmelting. Values found for different faces of β-Sn are moderately negative, and those for Cd are marginally positive. The search for surface nonmelting or melting on these metals should be interesting in light of these results.

I. INTRODUCTION

Melting and freezing of crystals is an area of continuing interest in condensed-matter physics. One particularly interesting topic concerns the beginning of the melting process at the crystal surface. It is well known that an extremely thin liquid layer appears on many crystals when the temperature is still a few degrees or tenths of a degree below the melting point (T_M). In most cases the thickness l of this layer grows sharply with increasing temperature, and extrapolates to an infinite value $l\rightarrow\infty$ at $T=T_M$ (surface melting). In other cases, l remains finite at T_M (blocked or incomplete surface melting), and in still other cases no liquid layer appears at all and the surface remains crystalline (surface nonmelting). Since the liquid layer is bounded by two interfaces, the solid-liquid interface and the liquid-vapor interface, one can attribute nonmelting and blocked melting to binding, and surface melting to unbinding, of the two interfaces. The thermodynamical forces which the two interfaces exert on one another act as an effective interface-interface potential $V(l)$. This effective potential consists of two conceptually distinct parts. One is a short-range part $V_{\rm SR}$, which is generally oscillatory, with minima corresponding to "monatomic layers," and which decays exponentially to zero for large l. This short-range effective interaction between the interfaces is related directly to short-range interatomic potentials (which have a hard core as well as an attractive well) plus additional thermal effects. The other part is a long-range interface-interface potential, which in the nonretarded limit has the asymptotic form $V_{\rm LR}=H/l^2$, and is due to dispersion electromagnetic forces. The constant H is the so-called Hamaker constant (sometimes also defined as $H'=12\pi H$),[1] and will form the main concern of this paper.

Surface melting, i.e., interface unbinding, takes place whenever the minima of $V_{\rm SR}(l)$ are not too deep, and, at the same time, long-range forces are *repulsive,* i.e., $H>0$. Conversely, interface binding, resulting in incomplete melting or nonmelting, may be due either to (a) trapping in the deep minima of $V_{\rm SR}(l)$ or to (b) *attractive* long-range forces $H<0$.

The Hamaker constant H tends to be generally positive, so that the nonmelting observed on special close-packed surfaces of metals such as Pb, Au, or Al (whose less packed surfaces are observed instead to melt), is due strictly to short-range forces. On the other hand, the Hamaker constant can occasionally be negative, typically when the liquid is denser than the solid, or a better conductor than the solid. If that happens for a cubic crystal, it necessarily implies nonmelting or blocked melting for all faces of that crystal. This was predicted in Ref. 2 for semiconductors such as Ge which contract and turn metallic upon melting.

However, many interesting systems in nature are noncubic, including some low-melting-point metals such as Hg, α-Ga, β-Sn, and Cd as well as vast classes of molecular crystals. What about them? Can one generalize the existing formulas for cubic crystals? Will the Hamaker constant remain a scalar property, as it is in the cubic case, or will it become face dependent? And, in that case, could we find a situation where $H>0$ for one face and $H<0$ for another face of the same crystal? It would be interesting to find a case where that occurs, since then one face would melt away but the other would not, creating unexpected geometries.

The purpose of this paper is precisely to present an answer to these questions. In addition, we shall attempt to estimate H for the main faces of α-Ga, β-Sn, and Cd based on the optical data found in the literature. The bottom line is that, while H does vary from face to face, it does not change sufficiently to imply a reversal of behavior among different faces of these few crystals. This leaves open the possibility that this could happen elsewhere. One of the aims of this paper is to suggest looking experimentally for this kind of situation.

Dispersion forces arise from a modification of quantum-mechanical zero-point electromagnetic fluctuations caused by the presence of two or more different media. A simple calculation of these forces can be done using the well-known theory of Lifshitz and coworkers,[3,4] whose input is the frequency-dependent dielectric functions $\epsilon(\omega)$ of the solid and liquid, both assumed to be isotropic. Based on existing optical data, this calculation was carried out, for example, by Chen, Levi, and Tosatti[2] for some cubic crystals (Pb, Al, Au, Ge). We shall extend the Lifshitz theory to treat a liquid layer on top of a crystal which has different dielectric constants [i.e., components of the dielectric tensor $\epsilon_{ij}(\omega)$] along different principal axes. We will suppose the solid surface to be normal or parallel to the optical axis for uniaxial crystals, and to contain two principal axes in the case of biaxial orthorhombic crystals (such as α-Ga) whose principal axes remain fixed in space as the frequency varies. More complicated geometries are not amenable to so simple a solution, and will not be discussed here.

This paper is organized as follows. In Sec. II, we generalize the Lifshitz formula using the formalism of thermal Green functions to treat electromagnetic fluctuations in anisotropic media. Equation (32) in this section is our main result. In Sec. III, we describe a crude interpolation procedure (the same as in Ref. 2) used to fit experimental data of dielectric constants for α-Ga, Cd, and β-Sn, and in Sec. IV we discuss the results obtained for the Hamaker constant of different faces of these crystals, using these dielectric functions and Eq. (36). A short discussion in Sec. V concludes the paper.

II. DISPERSION FORCES IN ANISOTROPIC SOLIDS

We consider two media A and B occupying the half-spaces $x<0$ and $x>l$. Between A and B there is a third medium C $(0<x<l)$. When the thickness l is much greater than the interatomic distances, macroscopic electrodynamics can be used to calculate the force between the two interfaces. The origin of this force is the same as that giving rise to the Van der Waals force between two noble-gas atoms. Fluctuations in the electromagnetic field of long wavelength give rise to a nonzero Maxwell stress tensor in all points of the interface among media B and C. We will compute the Maxwell stress tensor, restricting ourselves to the case where the thickness l is much smaller than the wavelength of the electromagnetic radiation which characterizes absorption spectra of the media. The electromagnetic properties of different media are described by their dielectric tensor, and we suppose that A is an anisotropic solid, B is a vapor (taken to have $\epsilon=1$-like vacuum), and C is an isotropic liquid.

Electromagnetic fluctuations in the media can be described in terms of thermal Green functions:[5]

$$D_{ij}(\mathbf{r}_1,\tau_1,\mathbf{r}_2,\tau_2)=-\langle T_\tau(A_i(\mathbf{r}_1,\tau_1)A_j(\mathbf{r}_2,\tau_2))\rangle , \quad (1)$$

where $\langle\ \rangle$ is the quantum thermal average in a canonical ensemble with temperature $1/\beta$, $A_i(\mathbf{r},\tau)$ is the ith component of the vector potential, and dependence on the imaginary time τ is obtained in the usual way from the corresponding Schrödinger operator:

$$A_i(\mathbf{r},\tau)=e^{H\tau/\hbar}A_i(\mathbf{r})e^{-H\tau/\hbar} , \quad (2)$$

where H is the Hamiltonian of the medium plus electromagnetic field. We choose a radiation gauge where the scalar potential is zero, as appropriate for a charge-free problem. D_{ij} depends only on the difference $\tau_2-\tau_1$, and in the range $-\hbar\beta\le\tau_2-\tau_1\le\hbar\beta$ can be expanded in a Fourier series over the Matsubara frequencies:

$$D_{ij}(\mathbf{r}_1,\mathbf{r}_2,\tau_2-\tau_1)=\frac{1}{\beta}\sum_{n=-\infty}^{+\infty}D_{ij}(\xi_n,\mathbf{r}_1,\mathbf{r}_2)e^{i\xi_n(\tau_1-\tau_2)} , \quad (3)$$

where $\xi_n=2\pi n/\hbar\beta$. In terms of these Fourier components of D_{ij}, we can write the xx component of Maxwell's stress tensor at an arbitrary point $\mathbf{r}=(l,y,z)$ of the interface between media B and C:[5,6]

$$\sigma_{xx}(l)=\frac{1}{4\pi\beta}\sum_{n=0}^{\infty}{}'\{[D^E_{yy}+D^E_{zz}-D^E_{xx}]\epsilon_c(i\xi_n)+D^H_{yy}+D^H_{zz}-D^H_{xx}\} , \quad (4)$$

where all D are calculated at $\mathbf{r}_1=\mathbf{r}_2=(l,y,z)$ and at the frequency ξ_n; the quantities D^E and D^H can be obtained from D_{ik} by

$$D^E_{ik}=-\xi_n^2 D_{ik} ,$$
$$D^H_{ik}=\varepsilon_{isl}\varepsilon_{ktm}\frac{\partial}{\partial x_s^1}\frac{\partial}{\partial x_t^2}D_{lm} , \quad (5)$$

where ε_{ijk} is the completely antisymmetric Ricci tensor.

Thermal Green functions obey a set of differential equations that can be obtained using the relationship between the thermal Green function and the corresponding retarded function[5]

$$D_{ik}(\xi_s,\mathbf{r}_1,\mathbf{r}_2)=D^R_{ik}(i|\xi_s|,\mathbf{r}_1,\mathbf{r}_2) , \quad (6)$$

plus the fact that the retarded Green function is proportional to the generalized susceptibility which relates, in linear theory, the current to the induced potential field. We obtain

$$A_i(\omega,\mathbf{r})=-\frac{1}{\hbar c}\int D^R_{ik}(\omega,\mathbf{r},\mathbf{r}')j_k(\omega,\mathbf{r}')d^3r' . \quad (7)$$

Writing Maxwell equations for A_i, we obtain a set of equations for D^R_{ik} and an equivalent set for D_{ik}:

$$\left[\frac{\partial^2}{\partial x_i \partial x_l}-\delta_{il}\Delta+\frac{\xi_n^2}{c^2}\varepsilon_{il}(i|\xi_n|,\mathbf{r})\right]D_{lk}(\xi_n,\mathbf{r},\mathbf{r}_1) = -4\pi\hbar\delta_{ik}\delta(\mathbf{r}-\mathbf{r}_1)\ . \quad (8)$$

The dielectric tensor depends on $\mathbf{r}$, but is constant inside media A, B, and C. We suppose that the surface of medium A is perpendicular to a principal axis so we can write

$$\varepsilon_A=\begin{bmatrix}\varepsilon_{xx}(\omega) & 0 & 0\\ 0 & \varepsilon_{yy}(\omega) & 0\\ 0 & 0 & \varepsilon_{zz}(\omega)\end{bmatrix}, \quad (9)$$

while in the isotropic media B and C, ε is proportional to the unit tensor. This choice of ε fixes Cartesian axes to coincide with the principal axes of crystal A. We have to solve problem (8) separately in the three regions and then use boundary conditions to match solutions at the interfaces. In order to solve Eq. (8), we use Fourier transforms of D_{ik} in the y and z directions, where the system is homogeneous, and calculate the functions which enter in the Maxwell stress tensor as

$$D_{ik}(\xi_n,\mathbf{r},\mathbf{r})=\int\frac{d^2k}{(2\pi)^2}D_{ik}(\xi_n,k_y,k_z,x,x)\ . \quad (10)$$

It is convenient to transform to a new reference system chosen such that the y axis is parallel to the $\mathbf{k}$ direction. The dielectric tensor $\tilde{\varepsilon}$ obtained by rotating around the x axis by an angle ϑ,

$$\cos\vartheta=\frac{k_y}{q},\quad \sin\vartheta=\frac{k_z}{q},\quad q=\sqrt{k_z^2+k_y^2}\ , \quad (11)$$

is of the form

$$\tilde{\varepsilon}=\begin{bmatrix}\varepsilon_{xx} & 0 & 0\\ 0 & \varepsilon_{yy}\cos^2\vartheta+\varepsilon_{zz}\sin^2\vartheta & (\varepsilon_{zz}-\varepsilon_{yy})\sin\vartheta\cos\vartheta\\ 0 & (\varepsilon_{zz}-\varepsilon_{yy})\sin\vartheta\cos\vartheta & \varepsilon_{yy}\sin^2\vartheta+\varepsilon_{zz}\cos^2\vartheta\end{bmatrix}\equiv\begin{bmatrix}\varepsilon_{xx} & 0 & 0\\ 0 & \varepsilon_{yy}^t & \varepsilon_{yz}^t\\ 0 & \varepsilon_{yz}^t & \varepsilon_{zz}^t\end{bmatrix} \quad (12)$$

and $\mathbf{k}=(q,0)$. Using this expression, we can write explicitly Eq. (8) in medium A:

$$D_{xx}=-\frac{iq}{w_{xx}^2}\frac{d}{dx}D_{yx}\ ,$$

$$D_{xy}=-\frac{iq}{w_{xx}^2}\frac{d}{dx}D_{yy}\ ,$$

$$D_{xz}=-\frac{iq}{w_{xx}^2}\frac{d}{dx}D_{yz}\ ,$$

$$\frac{q^2-w_{xx}^2}{w_{xx}^2}\frac{d^2}{dx^2}D_{yy}+\frac{\xi^2}{c^2}\varepsilon_{yy}^t D_{yy}+\frac{\xi^2}{c^2}\varepsilon_{yz}^t D_{zy}=0\ , \quad (13)$$

$$\frac{\xi^2}{c^2}\varepsilon_{yz}^t D_{yy}+\left[-\frac{d^2}{dx^2}+w_{zz}^2\right]D_{zy}=0\ ,$$

$$\frac{q^2-w_{xx}^2}{w_{xx}^2}\frac{d^2}{dx^2}D_{yz}+\frac{\xi^2}{c^2}\varepsilon_{yy}^t D_{yz}+\frac{\xi^2}{c^2}\varepsilon_{yz}^t D_{zz}=0\ ,$$

$$\frac{\xi^2}{c^2}\varepsilon_{yz}^t D_{yz}+\left[-\frac{d^2}{dx^2}+w_{zz}^2\right]D_{zz}=0\ ,$$

where we have defined

$$w_{xx}^2=q^2+\frac{\xi^2}{c^2}\varepsilon_{xx}\ ,$$

$$w_{zz}^2=q^2+\frac{\xi^2}{c^2}\varepsilon_{zz}^t\ . \quad (14)$$

This is now a linear set of differential equations with constant coefficients. We look for a solution with exponential decay in the region $x<0$, that is,

$$D_{yy}=A_1e^{w_A x},\quad D_{zy}=A_2e^{w_A x}\ ,$$

$$D_{zz}=A_3e^{w_A x},\quad D_{yz}=A_4e^{w_A x}\ . \quad (15)$$

Substituting in Eq. (13), we obtain a linear homogeneous problem, and the condition of the nonzero solution produces the relation

$$w_A^4-w_A^2\left[\frac{\varepsilon_{yy}^t}{\varepsilon_{xx}}w_{xx}^2+w_{zz}^2\right]+\frac{\varepsilon_{yy}^t}{\varepsilon_{xx}}w_{xx}^2w_{zz}^2-\frac{\xi^2}{c^2}\frac{\varepsilon_{yz}^{t\,2}}{\varepsilon_{xx}}w_{xx}^2=0\ . \quad (16)$$

The solutions of this biquadratic equation are both positive:

$$w_\pm^2=\frac{1}{2}\left[\frac{\varepsilon_{yy}^t}{\varepsilon_{xx}}w_{xx}^2+w_{zz}^2\right]\pm\frac{1}{2}\left[\left[\frac{\varepsilon_{yy}^t}{\varepsilon_{xx}}w_{xx}^2-w_{zz}^2\right]^2+\frac{4\xi^2}{c^2}\frac{\varepsilon_{yz}^{t\,2}}{\varepsilon_{xx}}w_{xx}^2\right]^{1/2}, \quad (17)$$

yielding two positive values w_- and w_+. The general solution for A can be written in the form

$$D_{yy}=A_1e^{w_+x}+A_2e^{w_-x}\ ,$$

$$D_{xy}=A_3e^{w_+x}+A_4e^{w_-x}\ ,$$

$$D_{zz}=A_5e^{w_+x}+A_6e^{w_-x}\ , \quad (18)$$

$$D_{yz}=A_7e^{w_+x}+A_8e^{w_-x}\ .$$

Clearly, only four of the coefficients are independent because they are the solutions of the homogeneous problem. The relationship between them is

$$\varepsilon^t_{yz} A_{3,5} = \left[\frac{\varepsilon_{xx}}{w^2_{xx}} w^2_+ - \varepsilon^t_{yy} \right] A_{1,7} ,$$
$$\varepsilon^t_{yz} \frac{\xi^2}{c^2} A_{2,8} = (w^2_- - w^2_{zz}) A_{4,6} . \tag{19}$$

The linear problem (13) is also valid in media B and C, with $\varepsilon^t_{yz}=0$ and $\varepsilon_{xx}=\varepsilon_{yy}=\varepsilon_{zz}=\varepsilon_B$ or ε_C, which in our case is 1. In medium C, we have to consider also the inhomogeneous term on the right side of Eq. (8), because we want to calculate the Maxwell tensor in that region. In this case, equations containing D_{yy} and D_{zz} do not depend on D_{yz} and D_{zy}, and we can look for a solution which is the sum of solutions of the homogeneous system and of a particular solution of the complete problem:

$$D_{zz} = C_1 e^{w_c x} + C_2 e^{-w_c x} - \frac{2\pi\hbar}{w_c} e^{-w_c |x - x_1|} ,$$
$$D_{yy} = C_3 e^{w_c x} + C_4 e^{-w_c x} - \frac{2\pi\hbar c^2 w_c}{\xi^2 \varepsilon_c} e^{-w_c |x - x_1|} , \tag{20}$$

where, in analogy with Eqs. (14), $w_c^2 = q^2 + \xi^2/c^2\varepsilon_c$. In medium B there is no inhomogeneous term, and we have to consider only solutions of the homogeneous system which decay exponentially for $x \to +\infty$:

$$D_{zz} = B_1 e^{-w_B (x - l)} ,$$
$$D_{yy} = B_2 e^{-w_B (x - l)} . \tag{21}$$

In order to evaluate the unknown coefficients, we use boundary conditions at the interfaces between the three media. These matching conditions can be obtained from the differential set (8) by integrating over a small volume around the surface. They are analogous to the usual conditions for continuity of the tangential component of the electric field, and for the normal component of electric induction. We have to require continuity of

$$D_{zz}, \quad D_{yy}, \quad \frac{d}{dx} D_{zz}, \quad \frac{\varepsilon_{xx}}{w^2_{xx}} \frac{d}{dx} D_{yy} . \tag{22}$$

In this general form we consider also the conditions for D_{yz} and D_{zy}, and we obtain two 8×8 sets where the two off-diagonal 4×4 matrices have almost all zero elements. However, here we are interested only in the solutions for the case in which the wavelength of the fluctuations which give rise to a nonzero Maxwell stress tensor are much longer than the distance between the two surfaces. In this case, we can simplify the set to obtain two 4×4 subsets that are completely separated. A typical case for the validity of this approximation is the surface of a metal whose absorption peaks are in the infrared or visible range of the spectrum, while the thickness of the liquid layer can be in the range between 10 and 100 Å. In this particular limit, we can approximate w_c, w_{xx}, w_{zz} using the fact that

$$q^2 \gg \frac{\xi^2}{c^2} \varepsilon \tag{23}$$

for all frequencies of interest. If we measure w_c in units of $(\xi^2/c^2)\varepsilon_c$, we can write

$$w_c^2 = \frac{\xi^2}{c^2} \varepsilon_c p^2 \quad \text{where } p \gg 1 , \tag{24}$$

an analogous relation for w_{xx} and w_{zz}. If we solve this equation for q (which is contained in w_c), and we insert the resulting expression into Eq. (19), we obtain, in the limit of $p \gg 1$,

$$w_+ = \left[\frac{\varepsilon^t_{yy}}{\varepsilon_{xx}} \varepsilon_c \frac{\xi}{c} p \right]^{1/2} ,$$
$$w_- = \sqrt{\varepsilon_c} \frac{\xi}{c} p , \tag{25}$$

and $A_2 = A_3 = A_5 = A_8 = 0$. This shows that in this limit D_{zz} and D_{yy} are independent from D_{yz} and D_{zy}. In this way we can solve the set for the coefficient exactly as in the isotropic case. Inserting the values of the coefficients into Eq. (20), we obtain an expression of D_{ij} which diverges for $x = x_1$. This divergence takes place at short wavelengths and is due to the fact that the present macroscopic theory cannot be applied to wavelengths comparable with atomic dimensions. The divergent term is therefore naturally cut off at atomic scale. However, this term gives no contribution to the Maxwell stress tensor, and for this reason we can eliminate it simply by subtracting from D_{ij} the divergent part D^0_{ij}, which is also present in vacuum and can be calculated in the limit $\varepsilon_A = \varepsilon_B = 1$. The final solution is for D_{yy}:

$$D_{yy} = \frac{2\alpha_1}{\Delta_1} \cosh w_c (x - x_1) , \tag{26}$$

where

$$\alpha_1 = \frac{2\pi\hbar w_c c^2}{\xi^2 \varepsilon_c} , \tag{27}$$

$$\Delta_1 = 1 - e^{2w_c l} \frac{\left[\frac{\varepsilon_c}{w_c} + \frac{\varepsilon_{xx}}{w^2_{xx}} w_+ \right] \left[\frac{\varepsilon_c}{w_c} + \frac{1}{w_B} \right]}{\left[\frac{\varepsilon_c}{w_c} - \frac{\varepsilon_{xx}}{w^2_{xx}} w_+ \right] \left[\frac{\varepsilon_c}{w_c} - \frac{1}{w_B} \right]} , \tag{28}$$

and, for D_{zz},

$$D_{zz} = \frac{2\alpha}{\Delta} \cosh w_c (x - x_1) , \tag{29}$$

where

$$\alpha = \frac{2\pi\hbar}{w_c} , \tag{30}$$

$$\Delta = 1 - e^{2w_c l} \frac{(w_{zz} + w_C)(w_B + w_C)}{(w_{zz} - w_C)(w_B - w_C)} . \tag{31}$$

Using these expressions we can calculate D^E_{ik} and D^H_{ik}, to be inserted into the Maxwell stress tensor. In the limit of long wavelengths, the term arising from D_{zz} provides no contribution. We finally obtain the force acting between the two interfaces AC and CB bounding the liquid

layer in the form

$$F(l)=\frac{\hbar}{8\pi^2 l^3}\int_0^\infty d\xi \int_{-\pi}^{\pi}\frac{d\vartheta}{2\pi}\frac{[\sqrt{\varepsilon_{xx}\varepsilon_{yy}^t(\vartheta)}-\varepsilon_c](1-\varepsilon_c)}{[\sqrt{\varepsilon_{xx}\varepsilon_{yy}^t(\vartheta)}+\varepsilon_c](1+\varepsilon_c)} . \tag{32}$$

The dependence of $\varepsilon_{yy}^t(\vartheta)$ is derived from Eq. (12), which defines this quantity. Of course this final result is similar to the Lifshitz formula,[4] which is generalized in a simple way to include the angular dependence of the extraordinary ray dielectric function ε_{yy}^t.

In the case of a uniaxial solid with an optical c axis perpendicular to the surface, ε_{yy}^t does not depend on the angle ϑ, and the angular integration can be done immediately. The result in that case is that the isotropic dielectric constant of the solid in the Lifshitz formula must now be replaced by the *geometric average* of the dielectric constants in the directions parallel and perpendicular to the c axis. In a more general case, the effective solid dielectric constant is an approximate average of the various effective solid dielectric constants seen by each wave contributing to the force and propagating at a given angle with respect to the principal axes.

The physics of the above result can be interpreted easily in the case of a uniaxial crystal with the surface perpendicular to the optical axis. In this case, electromagnetic waves propagating in the medium factorized in an ordinary ray[7] whose dispersion relation is

$$q_x^2+q_y^2-\frac{\omega^2}{c^2}\varepsilon_{yy}=0 , \tag{33}$$

and an extraordinary ray,

$$\varepsilon_{xx}q_x^2+\varepsilon_{yy}q_y^2-\frac{\omega^2}{c^2}\varepsilon_{xx}\varepsilon_{yy}=0 . \tag{34}$$

The ordinary ray turns out not to contribute to the dispersion forces between the two interfaces. The only contribution comes from the extraordinary ray, whose effective dielectric function is precisely $\varepsilon_{xx}\varepsilon_{yy}$, which enters into Eq. (32).

Using Eq. (32) for the force between the two surfaces, we readily obtain the Hamaker constant from the relation

$$F(l)=\frac{2H}{l^3} . \tag{35}$$

It is clear from the above that, in general, the Hamaker constant is now face dependent, unlike the cubic case. We stress again that this simple result is possible only for the simple geometry that is assumed. In particular, we have not been able to obtain a simple result for a general face orientation and an arbitrary low crystal symmetry. In that case, the set Eq. (8) cannot be simply factorized in 4×4 independent subsets, and the solution for D_{ij} is much more involved.[8]

III. PROCEDURE FOR PRACTICAL CALCULATIONS

In order to compute numerically the Hamaker constant

$$H=\frac{\hbar}{16\pi^2}\int_0^\infty d\xi \int_{-\pi}^{\pi}\frac{d\vartheta}{2\pi}\frac{[\sqrt{\varepsilon_{xx}\varepsilon_{yy}^t(\vartheta)}-\varepsilon_c](1-\varepsilon_c)}{[\sqrt{\varepsilon_{xx}\varepsilon_{yy}^t(\vartheta)}+\varepsilon_c](1+\varepsilon_c)} , \tag{36}$$

we need *analytical* expressions for the principal dielectric functions of the solid and the liquid, to be continued for imaginary values of the frequency. However, what is available in practice is, in the best case, a limited set of numerical data, usually optical studies of the dielectric functions. There are several published measurements of these quantities in the range between 0 and 5 eV, which is the range of frequency which gives the most important contribution to Eq. (32). The numerical accuracy of the result will surely be influenced by the lack of information about the higher frequencies. However, in this work we intend principally to explore sign, and to obtain an idea of the difference of the Hamaker constant in different surfaces of the same solid. For this limited purpose, an interpolation procedure is probably sufficient to account for the high-frequency contribution. We have interpolated these data with a Drude model. The details of the interpolation procedure are the same as in Ref. 2. Here we summarize only the most important formulas. Each component of the dielectric tensor of the solid is written as a sum of oscillators:

$$\varepsilon(\omega)=1+\omega_p^2\sum_m\frac{f_m}{\omega_m^2-\omega^2-i\Gamma_m\omega} . \tag{37}$$

Here ω_p is the plasma frequency of the medium, ω_m are the frequencies of the interband transitions, each of oscillator strength f_m fulfilling the f-sum rule

$$\sum_m f_m=1 . \tag{38}$$

For a metal, there is a pole at $\omega=0$, and from the sum over the poles we can extract the intraband absorption Drude term

$$\varepsilon^{\text{intra}}(\omega)=-\frac{f^{\text{intra}}\omega_p^2\tau}{\omega^2\tau+i\omega} . \tag{39}$$

From experimental optical data, we obtain the values of the resonance frequencies ω_m, of their linewidths Γ_m, and of the oscillator strengths f_m. The value of the intraband relaxation time τ can be obtained by fitting the static conductivity in the form

$$\sigma(\omega)=\frac{\sigma_0}{(1+\omega^2\tau^2)} . \tag{40}$$

We can then fix f^{intra} from the relation

$$\sigma_0=f^{\text{intra}}ne^2\tau/m . \tag{41}$$

We shall apply this procedure to orthorhombic α-Ga, to tetragonal β-Sn, and to hexagonal Cd. Experimental data for gallium are given near the melting point, so that they can be used without modification. For cadmium and tin, we have to extrapolate the room-temperature data to the melting point. We do this by correcting only the value of τ to fit the conductibility at the melting point. Liquid

dielectric constants are also available,[9] and are generally fitted by a Drude formula with reasonable accuracy. We therefore assume that in the liquid there is no strong interband transition, and we estimate the plasma frequency from the valence electron density, and the value of τ from the static conductivity.

IV. HAMAKER CONSTANTS

A. Hamaker constants of gallium surfaces

α-Ga is an orthorhombic, biaxial crystal.[10] Its principal axes are perpendicular to the faces of the elementary cell. Dielectric functions of solid gallium have been measured[11] in the range 0.5–3 eV and are reported in Fig. 1 as points. Solid curves represent our interpolations. There are three valence electrons, giving both a Drude-like metallic contribution at low frequencies and covalent interband peaks near 1.0 and (more importantly) 2 eV. At room temperature, α-Ga has a density $\rho_m = 5.91$ g/cm^3, corresponding to $r_s = 2.19$ and to a bulk plasma frequency $\hbar\omega_p = 14.5$ eV. Static resistivities of gallium are[12] $\rho_1 = 17.5$ $\mu\Omega$ cm (a axis), $\rho_2 = 8.1$ $\mu\Omega$ cm (b axis), and $\rho_3 = 53.3$ $\mu\Omega$ cm (c axis). The great differences in static resistivity along different directions reflect an even greater difference in the Drude oscillator strength f^{intra} in three directions. Fitting the optical data for $\omega \to 0$, we obtained $\tau_1/\hbar = 12.1$ eV^{-1}, $f_1^{\text{intra}} = 0.16$ (a axis), $\tau_2/\hbar = 12.7$ eV^{-1}, $f_2^{\text{intra}} = 0.33$ (b axis), $\tau_3/\hbar = 13.6$ eV^{-1}, and $f_3^{\text{intra}} = 0.05$ (c axis). This is in agreement with covalent bonds, making α-Ga nearly insulating in the c direction.[13]

In Table I, we report all the fitting parameters used to interpolate experimental results. We have added small fictitious absorption peaks at $\hbar\omega_m = 5.0$–7.0–9.0 eV, not really present in experimental data. These peaks are used to fulfill the sum rule (38), otherwise violated. The experimental data contain a certain margin of error, for which we attempt to compensate with these terms. On the other hand, they clearly introduce a source of error in our own calculation which we estimate to be of the order of 10%. Liquid gallium has a density $\rho_{ml} = 6.1$ g/cm^3, 3% larger than that of α-Ga. If we suppose that there remain three electrons per atom which participate in optical properties, this corresponds to a plasma frequency of $\hbar\Omega_p = 14.7$ eV. This hypothesis is experimentally checked in Ref. 9, where in addition it is shown that the optical properties of liquid gallium are entirely Drude-like. Thus we assume $f^{\text{intra}} = 1$ and use static resistivity $\rho_l = 26$ $\mu\Omega$ cm to estimate $\tau/\hbar = 1.31$ eV^{-1}. With these data, we obtain three values of the Hamaker constant for the three surfaces perpendicular to each principal axis:

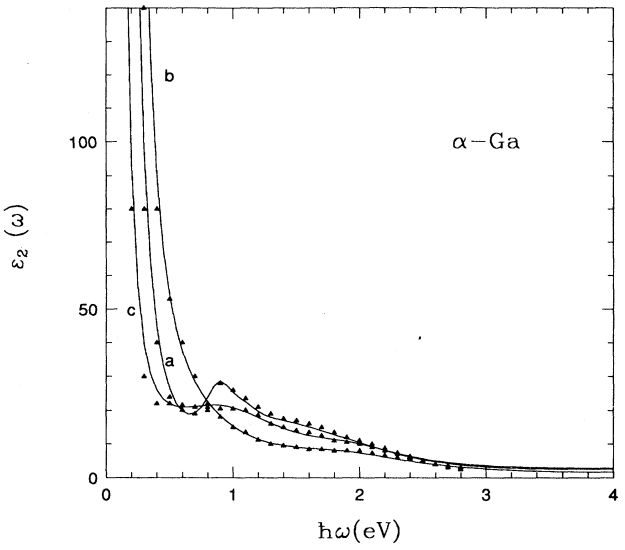

FIG. 1. A comparison between the imaginary part of the dielectric functions of Ga from experimental data at room temperature (triangles) and our fitted results (solid line), for the a, b, and c axes. The dielectric function is composed of a Drude peak at low frequencies and several peaks due to interband transition. The position of the peaks, their height and width are obtained with the procedure described in the text. Frequencies are expressed in eV.

TABLE I. Parameters used to fit a-, b-, and c-axis dielectric constants of gallium. ω_m, Γ_m, and f_m are defined in Eq. (37).

	$m=1$	$m=2$	$m=3$	$m=4$	$m=5$	$m=6$	$m=7$
a axis							
$\hbar\omega_m$ (eV)	0.9	1.1	1.5	2.0	6.0	7.0	9.0
$\hbar\Gamma_m$ (eV)	0.3	0.35	1.1	1.2	4.0	4.0	4.0
f_m	0.02	0.01	0.08	0.05	0.22	0.24	0.24
b axis							
$\hbar\omega_m$ (eV)	0.8	2.0	2.6	6.0	7.0	9.0	
$\hbar\Gamma_m$ (eV)	1.2	1.5	2.0	2.5	3.0	4.0	
f_m	0.05	0.07	0.01	0.1	0.12	0.32	
c axis							
$\hbar\omega_m$ (eV)	0.4	0.6	1.1	2.0	6.0	7.0	9.0
$\hbar\Gamma_m$ (eV)	2.5	1.3	1.25	1.1	5.0	5.0	4.0
f_m	0.02	0.01	0.02	0.05	0.2	0.27	0.28

(100) face (a axis): $H=-2.7\pm0.2\times10^{-21}$ J ,

(010) face (b axis): $H=-2.5\pm0.2\times10^{-21}$ J ,

(001) face (c axis): $H=-3.0\pm0.2\times10^{-21}$ J .

In all directions, we obtain a negative value of the Hamaker constant, and this requires nonmelting or at most blocked melting for (100), (010), and (001) surfaces (and probably all other faces) of α-Ga.

B. Hamaker constants of tin surfaces

β-Sn is a tetragonal uniaxial crystal[10] with four valence electrons and electronic structure (Kr) $4d^{10}5s^25p^2$. Its density $\rho_m=7.31$ g/cm^3 corresponds to $r_s=2.2$ and to a plasma frequency of $\hbar\Omega_p=14.3$ eV. The optical axis is perpendicular to the square face of the elementary cell. The static resistivity[12] at $T=293$ K in the direction parallel to the optical axis is $\rho_{\parallel}=14.3$ $\mu\Omega$ cm, while in the normal direction it is $\rho_{\perp}=9.85$ $\mu\Omega$ cm. Fitting optical data, for intraband parameters we obtained $\tau_{\parallel}/\hbar=6.0$ eV^{-1}, $f_{\parallel}^{\rm intra}=0.41$, $\tau_{\perp}/\hbar=7.9$ eV^{-1}, and $f_{\perp}^{\rm intra}=0.46$.

Dielectric constants have been reported in Ref. 14 in the range 0.5–5.5 eV and are shown in Fig. 2 along with our interpolation, described by the parameters of Table II. Clearly visible is the importance of interband transitions at $\hbar\omega_m=1.3$ eV and also in the range 3–5 eV, still present at room temperature. The melting point of β-Sn is $T_m=505$ K, and we need a dielectric constant at a temperature near the melting point, so we leave $f^{\rm intra}$ unchanged and change the relaxation time τ to fit the statical resistivity which, at this temperature, increases to $\rho_{\parallel}=26.47$ $\mu\Omega$ cm in the parallel direction and $\rho_{\perp}=1.5$ $\mu\Omega$ cm perpendicular to optical axis. At the melting point the density is $\rho_m=7.19$ g/cm^3 corresponding to $\hbar\Omega_p=14.2$ eV. From these data, we obtained $\tau_{\parallel}/\hbar=3.3$ eV^{-1} and $\tau_{\perp}/\hbar=4.6$ eV^{-1}.

Optical properties of liquid tin are reported in Ref. 12, and can be fit by a Drude model with 4.4 valence electrons every atom. With a density of liquid tin of $\rho_{ml}=7$ g/cm^3, we obtained a plasma frequency $\hbar\Omega_p=14.68$ eV, and, with a resistivity $\rho_l=47$ $\mu\Omega$ cm, a relaxation time $\tau/\hbar=0.73$ eV^{-1}. With these parameters we finally obtain

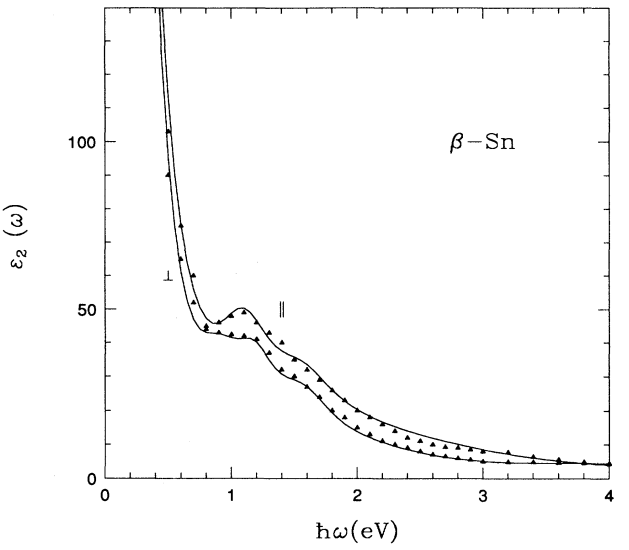

FIG. 2. A comparison between the imaginary part of the dielectric functions of Sn from experimental data at room temperature (triangles) and our fitted results (solid line), in directions parallel and perpendicular to the c axis. Frequencies are expressed in eV.

(100),(010)faces: $H=-0.38\pm0.1\times10^{-21}$ J ,

(001) face: $H=-0.45\pm0.1\times10^{-21}$ J .

The difference of the two Hamaker constants is very small, similar to our numerical error. The negative sign indicates either blocked surface melting or nonmelting. However, the value is one order of magnitude smaller than that of α-Ga and tendencies to nonmelting should be weaker in β-Sn. It should be interesting to check experimentally the true behavior of β-Sn surfaces, in the light of these results.

C. Hamaker constants of cadmium surfaces

Cadmium is a uniaxial hexagonal crystal[10] with two valence electrons and electronic structure (Kr) $4d^{10}5s^2$. Its density is $\rho_m=8.64$ g/cm^3, corresponding to $r_s=2.59$ and to a plasma frequency of $\hbar\Omega_p=11.3$ eV. The optical c axis is normal to the hexagonal face of the elementary cell. The static resistivity[12] along the c axis is $\rho_{\parallel}=8.56$

TABLE II. Parameters used to fit dielectric constants of tin. ω_m, Γ_m, and f_m are defined in Eq. (37). $\parallel$ refers to the c axis while $\perp$ is a direction perpendicular to the c axis.

	$m=1$	$m=2$	$m=3$	$m=4$	$m=5$	$m=6$	$m=7$
$\parallel$ axis							
$\hbar\omega_m$ (eV)	0.6	1.13	1.6	2.2	3.0	5.0	
$\hbar\Gamma_m$ (eV)	0.5	0.55	0.7	1.5	2.0	2.0	
f_m	0.01	0.09	0.09	0.12	0.1	0.08	
$\perp$ axis							
$\hbar\omega_n$ (eV)	0.9	1.0	1.2	1.6	2.2	4.0	5.5
$\hbar\Gamma_m$ (eV)	0.4	0.4	0.43	0.6	1.5	2.0	2.0
f_m	0.02	0.01	0.05	0.07	0.08	0.14	0.17

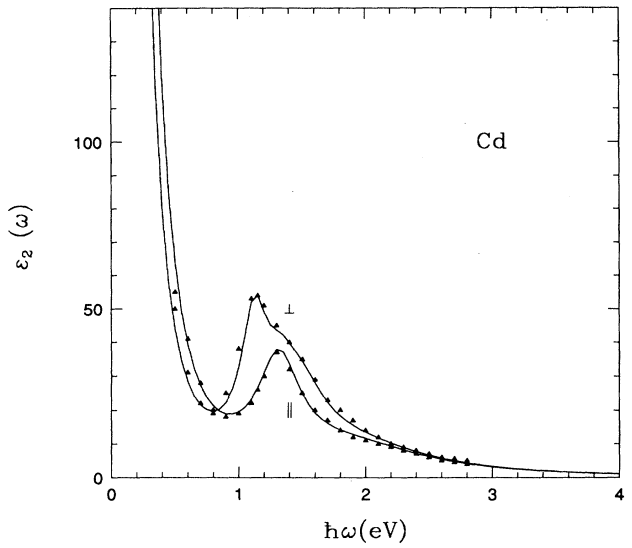

FIG. 3. A comparison between the imaginary part of the dielectric functions of Cd from experimental data at room temperature (triangles) and our fitted results (solid line), in directions parallel and perpendicular to the c axis. Frequencies are expressed in eV.

$\mu\Omega$ cm, while in the normal direction it is $\rho_\perp = 6.94$ $\mu\Omega$ cm. Fitting the optical spectra reported in Ref. 15 at low frequencies $\hbar\omega = 0.5$ eV, for intraband parameters we obtained the values $\tau_\perp/\hbar = 14.4$ eV^{-1}, $f_\perp^{\text{intra}} = 0.58$ and $\tau_\parallel/\hbar = 10.43$ eV^{-1}, $f_\parallel^{\text{intra}} = 0.65$.

The experimental dielectric constant and the interpolated curves are shown in Fig. 3, and the fitting parameters are reported in Table III. The melting point of cadmium is $T_M = 594$ K, and at this temperature density is $\rho = 8.4$ g/cm^3, corresponding to $\hbar\Omega_p = 11.1$ eV. Static resistivities become $\rho_\parallel = 18.37$ $\mu\Omega$ cm in the parallel direction, and $\rho_\perp = 15.47$ $\mu\Omega$ cm in the direction perpendicular to the optical axis. These parameters correspond to $\tau_\parallel/\hbar = 5.02$ eV^{-1} and $\tau_\perp/\hbar = 6.68$ eV^{-1}. We did not find data for the optical properties of liquid cadmium, so we merely supposed a Drude-like form with a relaxation time $\tau/\hbar = 1.86$ eV^{-1} corresponding to a measured resistivity $\rho_l = 34$ $\mu\Omega$ cm. Plasma frequency is $\hbar\Omega_p = 10.9$ eV, corresponding to a liquid cadmium density of $\rho_l = 8.02$ g/cm^3, and with these parameters we obtained

TABLE III. Parameters used to fit dielectric constants of cadmium. ω_m, Γ_m, and f_m are defined in Eq. (37).

	$m=1$	$m=2$	$m=3$	$m=4$
∥ axis				
$\hbar\omega_m$ (eV)	1.33	2.0		
$\hbar\Gamma_m$ (eV)	0.4	1.5		
f_m	0.12	0.23		
⊥ axis				
$\hbar\omega_m$ (eV)	1.13	1.33	1.5	2.0
$\hbar\Gamma_m$ (eV)	0.25	0.3	0.5	1.5
f_m	0.08	0.04	0.1	0.2

(100),(010)faces: $H = 0.12 \pm 0.1 \times 10^{-21}$ J ,

(001) face: $H = 0.096 \pm 0.1 \times 10^{-21}$ J .

These values are very small, and similar to our estimated error. Therefore we cannot really predict whether surface melting will be blocked or not. All we can conclude in this case is that the effect of long-range forces is expected to be small, and Cd should constitute a good test case for a system with essentially only short-range forces.

V. DISCUSSION

We have presented in Sec. II a generalization of Lifshitz's formulation of dispersion forces between planar media, in the case where one of the media is anisotropic. Our main result is Eq. (32) of Sec. II, showing that, in the long-wavelength limit, Lifshitz's result can be modified by simply substituting the solid isotropic dielectric function with an appropriate average of the components of the dielectric tensor.

Subsequently we have applied this result to a calculation of the long-range effective potential $V_{\text{LR}} = H/l^2$ between the solid-liquid and the liquid-vapor interfaces a distance l apart. As soon as the solid is anisotropic, the Hamaker constant H becomes face dependent. This has important consequences for surface melting, which is controlled by this constant, being enhanced by $H > 0$ and suppressed by $H < 0$.

Using dielectric functions obtained by approximate fitting of optical data, we have estimated the Hamaker constant for a few low-melting-point anisotropic metals, hoping to find one where $H > 0$ on one face and $H < 0$ on another. Unfortunately, none of the cases studied (α-Ga, β-Sn, and Cd) turns out to do that. All the same, the results are of some interest, suggesting the following separate comments.

α-Ga

For α-Ga, we find all surfaces to have large and negative H. Physically this is due to the solid being largely covalent and only partly metallic, as opposed to the more metallic and less covalent liquid. Our prediction of strong nonmelting is compatible with recent scanning tunneling microscopy (STM) studies,[16] indicating an exceptional tendency of most surfaces to remain stable and avoid surface melting. However, a negative Hamaker constant cannot really be blamed for surface stability down to the monolayer level. Therefore, in this regime, some kind of different mechanism involving short-range forces must be responsible for the generalized lack of surface melting, which is observed by STM and remains somewhat mysterious.

β-Sn

In β-Sn we also find all Hamaker constants to be negative, but one order of magnitude smaller than in α-Ga. It is therefore predicted that blocked melting is likely to take place, at least on the poorly packed faces (the well-packed face is likely not to melt at all, as usual, due to short-range forces). There are, as far as we know, no data

available for the surface melting habits of β-Sn, and it is clearly desirable to have some in the future. One interesting feature to check in the case of blocked melting of a poorly packed face will be the growth of the quasiliquid layer up to some finite maximum value l_{max} similar to that reported by Elbaum and Schick on the surface of ice.[17] Since this is due to a compromise between short-range forces, which push the solid-liquid and liquid-vapor interfaces apart, and long-range forces, which eventually keep them bound, it is not possible at this stage, where we have no idea of the actual short-range forces, to estimate l_{max}.

Cd

In this case, both Hamaker constants are marginally positive—or, better, basically zero, taking into account our very limited accuracy. The most we can say is that Cd should represent the best example of a crystal whose surface melting habit should be totally determined by short-range forces. Experimentally, Cd(0001) was historically the first surface to be seen by Mutaftschiev in the 1960s (Ref. 18) to exhibit what we now call nonmelting. If other faces do melt, as is likely, the growth of $l(T)$ should remain characteristically logarithmic to very large values of l, as expected for a system with short-range forces only.

ACKNOWLEDGMENTS

We are grateful to X. J. Chen for his help. This work was supported by INFM.

[1]J. N. Israelachvili, *Intermolecular and Surface Forces* (Academic, San Diego, 1985).
[2]X. J. Chen, A. C. Levi, and E. Tosatti, Nuovo Cimento **13**, 919 (1991).
[3]E. M. Lifshitz, Zh. Eksp. Teor. Fiz. **29**, 94 (1955) [Sov. Phys. JETP **2**, 73 (1956)].
[4]L. D. Landau and E. M. Lifshitz, *Electrodynamics of Continuous Media* (Pergamon, New York, 1960).
[5]E. M. Lifshitz, and L. P. Pitaevskii, *Fisica Statistica* (Editori Riuniti, Rome, 1981), Vol. 2.
[6]I. E. Dzyaloshinskiĭ and L. P. Pitaevskiĭ, Zh. Eksp. Teor. Fiz. **36**, 1797 (1959) [Sov. Phys. JETP **9**, 1282 (1959)].
[7]M. Born and E. Wolf, *Principles of Optics* (Pergamon, London, 1959).
[8]A more general approach to the problem has been discussed in a different context by J. Bernasconi, S. Strässler, and H. R. Zeller, Phys. Rev. A **22**, 276 (1980).
[9]N. R. Comins, Philos. Mag. **25**, 817 (1972).
[10]R. W. G. Wyckoff, *Crystal Structures* (Krieger, Malabar, FL, 1982), Vol. 1.
[11]R. Kofman, P. Cheyssac, and J. Richard, Phys. Rev. B **16**, 5216 (1977).
[12]J. Bass, in *Electrical Resistivity of Pure Metals and Dilute Alloys,* edited by K. H. Hellwege and O. Madelung, Landolt-Börnstein, New Series, Group X, Vol. III, Pt. 15a (Springer-Verlag, Berlin, 1985).
[13]X. G. Gong, G. Chiarotti, M. Parrinello, and E. Tosatti, Phys. Rev. B **43**, 14 277 (1991).
[14]H. Schwarz, Phys. Status Solidi B **44**, 603 (1971).
[15]R. J. Bartlett, D. W. Lynch, and R. Rosei, Phys. Rev. B **3**, 4074 (1971).
[16]O. Züger, Ph.D. thesis, Eidgenössische Technische Hochschule, 1992; O. Züger and U. Dürig, Phys. Rev. B **46**, 7319 (1992).
[17]M. Elbaum and M. Schick, Phys. Rev. Lett. **66**, 1713 (1991).
[18]B. Mutaftschiev and J. Zell, Surf. Sci. **12**, 317 (1968).